

Modeling and Analyzing for Human Body Blockage in Millimeter Wave at 28 GHz in Crowded Indoor Environment

Hongmei Zhao¹, Huikun Xu¹, Jielei Zhao¹, Xuebin Li¹, Kunfeng Shi¹

¹*School of Electric and Information Engineering, Zhengzhou University of Light Industry, Zhengzhou 450002, China*

Keywords: Millimeter wave, Crowded indoor environment, Channel parameters, Transmitter height.

Abstract: Millimeter wave (mm-wave) communication is a promising way of wireless communication in the future. This paper analyses mm-wave propagation characteristics, including path loss, shadow fading and delay spread at 28GHz in a crowded meeting room scenario. In order to obtain more realistic simulation results, we consider the electromagnetic parameters of human skin and clothes. At the same time, we set different transmitter (TX) heights and compare the influence of different TX heights on channel parameters. The result shows that path loss and delay spread would be increased due to the existence of human body blockages. With the increase of TX heights, the path loss factor n would be decreased. All routes shadow fading obey the normal distribution system with a mean of 0. This paper provides a theoretical guiding for the design of wireless communication system in a crowded indoor environment.

1 INTRODUCTION

With the proliferation of smart phones and other wireless user devices, a heavy increase of requirement for communication capacity and data transmission rate are predicted (Islam et al., 2016). How to provide more sufficient capacity to satisfy users' requirement is an urgent problem to solve, especially in a crowded environment. Now, high-frequency bands above 6 GHz start to catch people's eyes (Nakamura et al., 2017). Mm-wave (30-300GHz) is regarded as a promising frequency band to meet the needs of users. Mm-wave can provide unprecedented bandwidth, however, the main concern is that propagation paths cannot bypass obstacles so that there are blockages caused by human bodies and other objects, which could reduce signal strength. The propagation paths are mainly expected to be blocked by human bodies in a very crowded area like meeting room, stadium and so on. Clothes of different materials will also have an influence on channel characteristics, furthermore, different transmitter (TX) heights will also lead to different path loss.

The TX usually plays an important role in system performance during mm-wave propagation. (Maccartney et al., 2017), (Bai et al., 2018) compare the mm-wave system performance of

different antenna types. (Bile et al., 2018) has done some researches to evaluate the influence of distributed antennas on system performance in an indoor meeting room, when TX number is from 1 to 4, spatial distribution of signal coverage become more homogeneous. The line-of-sight path is expected to last longer as the number of TX increases, in other words, the adoption of distributed TX settings can reduce the probability of blockages occurring. But it does not consider the effect of changes in TX height. The work in (Gapeyenko et al., 2016) has shown that blocking probability increases with human density and separation between TX and receiver (RX) pairs. In addition, it analyses the relationship between path loss and distance between TX and RX. Furthermore, it demonstrates the existence of the optimal TX height. However, there are few studies about the influence of height change of on channel parameters, especially in such a crowded meeting room where human occupancy rate is 100%.

Based on the theory of Shooting and Bouncing Ray(SBR) method, this paper simulates a crowded meeting room by Wireless InSite software and gets channel parameters, including path loss, shadow fading and delay spread at 28GHz. This paper is organized as follows. Section 2 describes the simulation environment including simulation scenario, TX and RX parameters. In Section 3,

human body blockage effects are studied at 28GHz in a crowded meeting room scenario where human occupancy rate is 100%, the worst case for communication. We also do some researches on the influence of different TX heights on channel parameters. And Section 4 provides concluding remarks of this paper.

2 SIMULATION ENVIRONMENT

2.1 Scenario Model

We build a simulation scenario similar to an indoor meeting room where human occupancy rate is 100%, as shown in Figure 1(a). This meeting room includes a platform, an air conditioner, 100 chairs, 100 people, three glass windows and two metal doors. The study area is about 7m×11m×2.8 m. The floor is wooden floor, wall is gesso brick wall that thickness is 0.3m. The human body and chair are shown in Figure 1(b). The human body is consist of several different rectangle parts, including head, upper body, arms, thighs and calves, the detail sizes are shown in Table 1. In addition, we also consider properties of clothes materials. All the human bodies wear randomly the electromagnetic parameters clothes including cotton, red leather and yellow leather. The permittivity of the materials in this simulation at 28GHz is listed in Table 2 (Chahat et al., 2011), (Harmer et al., 2008).

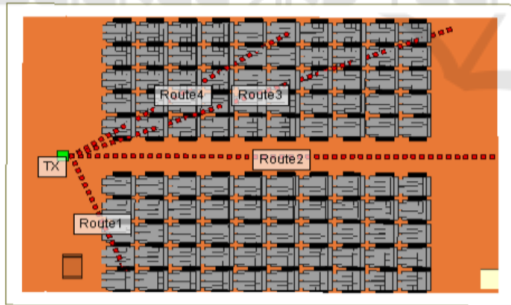


Figure 1 (a): 3D model for study area.

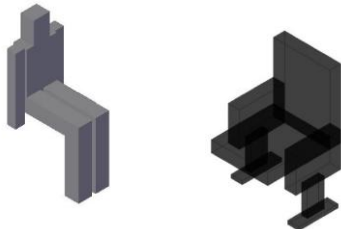


Figure 1(b): 3D model for human body and chair.

Table 1: The size of human body.

	length/height (cm)	width(cm)	Thickness (cm)
Head	20	15	10
Supper body	55	45	10
Thigh	52	15	10
Calf	48	15	10
Arm	60	10	10

Table 2: Materials property parameters.

Materials	Relative permittivity ϵ_y	Conductivity σ (S/m)
Dry wall	3.58	0.11
Glass	6.06	0.35
Gesso	2.02	/
Melamine board	4.7	/
Metal	/	∞
Cotton	1.7	0.038
Red leather	2.15	0.14
Yellow leather	2.3	0.09
Skin	10.05	7.32

2.2 Design on TX/RX

There are 3 TX (3.5m, 1m, 1.2/1.6/2.2m) which are located in the front of the meeting room. Four receive routes are shown in Figure 1 (a), Route1, Route2, Route3, Route4; All RX heights are 0.9 m, in order to study the spatial distribution of the delay spread, the RX also distribute in grid throughout the interior, and spacing is 0.2m. The gain of TX is 25dBi and the transmitted power is 10dBm. The relevant parameters of TX and RX are shown in Table 3.

Table 3: Simulation setup of TX and RX.

	TX	RX
Height (m)	1.2/1.6/2.2	0.9
Transmitted power (dBm)	10	/
Gain (dBi)	25	/
Antenna type	Omnidirectional	Omnidirectional
Frequency (GHz)	28	28
Polarization	Vertical-polarization	Vertical-polarization

3 RESULTS AND ANALYSIS

3.1 Path Loss

In general, the path loss model formula can be simply expressed as follows:

$$P = \frac{k}{d^n} \quad (1)$$

P represents the average envelope power, k is the scaling factor, d is distance between the transceivers, n is the path loss factor.

The simplified path loss model formula is also as follows:

$$P_R[dBm] = P_T[dBm] + K[dB] - 10 \cdot n \cdot \log_{10}\left(\frac{d}{d_0}\right) \quad (2)$$

P_R represents the received power (mw), P_T represents the transmitted power (mw), d_0 is the reference distance, in general, $d_0=1m$. K is usually the free space path gain at d_0 , where:

$$K = PG(d_0) = -PL(d_0) \quad (3)$$

Bring (3) into (2):

$$P_R[dBm] = P_T[dBm] - PL(d_0) - 10 \cdot n \cdot \log_{10}\left(\frac{d}{d_0}\right) \quad (4)$$

Transforming the truth value of path loss to dB, which is the dB difference between P_T and P_R , where:

$$PL(d) = 10\log_{10}\left(\frac{P_T}{P_R}\right) \quad (5)$$

Bring (4) into (5), and express it in logarithmic form by taking logarithm on both sides,

$$PL(d) = PL(d_0) + 10 \cdot n \cdot \log_{10}\left(\frac{d}{d_0}\right) \quad (6)$$

Considering the uncertainty of the realistic wireless communication environment, and various shades complicate the environment so that received signal is a superposition of multipath signal including reflection, diffraction, penetration and so on; especially in crowded indoor areas, more multipath components are present. There is always a

mixed model between path loss and shadow fading, where:

$$PL(d) = PL(d_0) + 10 \cdot n \cdot \log_{10}\left(\frac{d}{d_0}\right) + X_\sigma \quad (7)$$

X_σ represents a Gaussian random variable with mean μ and variance σ^2 .

We can obtain path loss data of receive Route1 when the TX height is 1.2m at 28 GHz by Wireless InSite, for getting $PL(d_0)$ and path loss factor n ; let $PL(d) = Y$, $PL(d_0) = a$, $10\log_{10}\left(\frac{d}{d_0}\right) = x$. When considering N pairs of observations (x_1, Y_1) , $(x_2, Y_2), \dots, (x_n, Y_n)$, the formula (7) should be changed as follows:

$$Y_i = a + nx_i + X_{\sigma i} \quad (8)$$

$X_{\sigma i}$ represents random deviation of the i^{th} observation. Next, regression analysis is carried out on the obtained data from Wireless InSite by using the least square method, $a=57.31$, $n=2.51$, Figure 2 describes the scatter-fitting line of Route1. Path loss model formula on Route1 for TX1 is:

$$PL(d) = 57.31 + 10 \cdot 2.51 \cdot \log_{10}\left(\frac{d}{d_0}\right) + X_\sigma \quad (9)$$

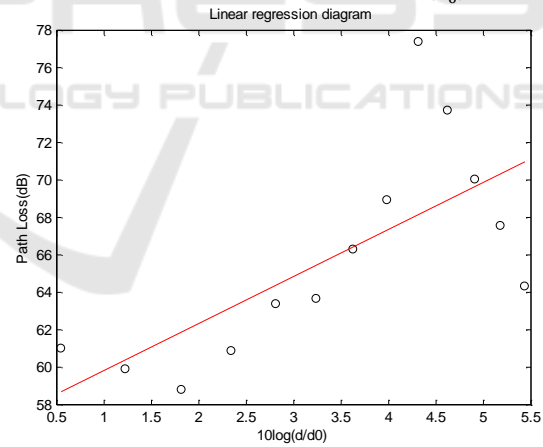


Figure 2: Route1 scatter-fitting line at TX1.

In order to evaluate the influence of different TX heights on channel characteristics, we keep TX two-dimensional position unchanged and set it into three different heights. TX1, TX2 and TX3 heights are 1.2m, 1.6m and 2.2m, respectively. The linear regression analysis of Route1-4 by least square method find that all 4 paths conform to the formula (7). $PL(d_0)$ and path loss factor n on Route1-4 at different TX heights obtained by regression analysis are shown in Table 4.

Table 4: Route1-4 $PL(d_0)$ and path loss factor n at different TX heights.

Route	$PL(d_0)$			n		
	TX1	TX2	TX3	TX1	TX2	TX3
Route1	57.31	59.99	75.86	2.51	1.50	-
Route2	59.29	61.75	68.06	1.86	1.48	0.98
Route3	48.89	57.31	62.44	3.84	2.31	1.35
Route4	57.81	65.69	78.04	2.43	0.94	-
						1.22

From Table 4, we find that as the increase of TX height, all Route1-4 $PL(d_0)$ are increased. And all path loss factor n are decreased. When TX height is 1.2m, Route2 path loss factor n is less than freedom space path loss factor ($n=2$), however, Route1, Route3 and Route4 path loss factor n are greater than 2. The reason for this phenomenon is that when the height of TX is 1.2m, Route2 is the line-of-sight path, however, Route1, Route3 and Route4 are blocked. In addition, Route3 has a more serious blockage so that its path loss factor n is greater than other routes whatever the TX height is. Route3 scatter-fitting lines at different TX heights are shown in Figure 3.

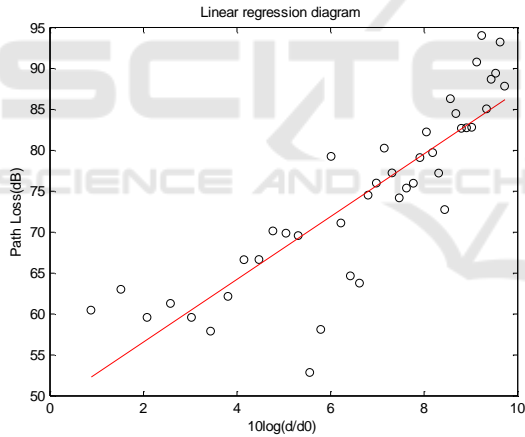


Figure 3(a): Route3 scatter-fitting line at TX1.

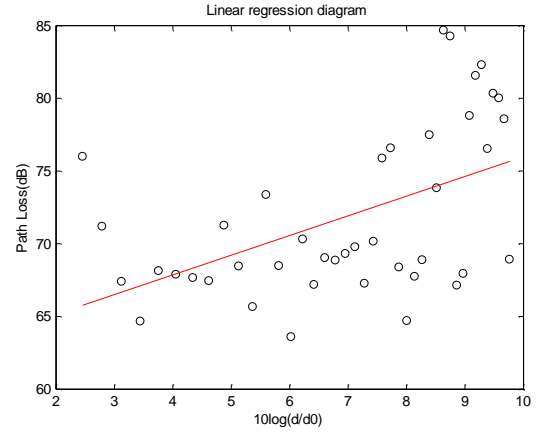
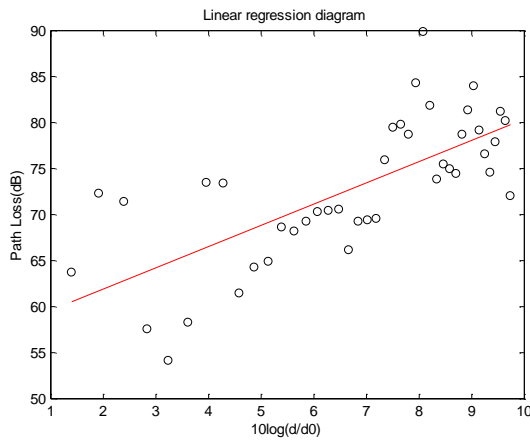


Figure 3(b): Route3 scatter-fitting line at TX2.

Figure 3(c): Route3 scatter-fitting line at TX3.

We can also know that when TX height is 2.2m, Route1 and Route4 path loss factor n both are negative by the Table 4. Route1 scatter-fitting lines are shown Figure 4.

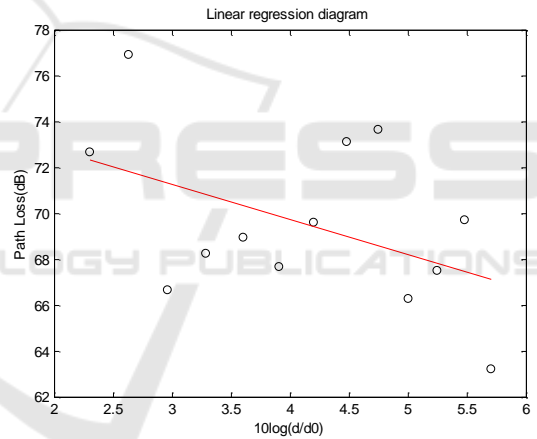


Figure 4: Route1 scatter-fitting line at TX3.

3.2 Shadow Fading

In part 3.1, we get a and n in the formula (8) by analysing fitting regression of four routes at different TX heights. However, $X_{\sigma i}$ is still unknown, and we will discuss more detail about it in order to verify the shadow fading distribution characteristics. When TX height is 1.2m, such as Route1 data, bring a and n into (8), which could get $X_{\sigma 1}, X_{\sigma 2}, \dots, X_{\sigma n}$. We mentioned it in part 3.1 that shadow fading obeys the normal distribution whose mean is μ and variance is σ^2 , so we have the assumption:

$$H: X_{\sigma} \sim N(\mu, \sigma^2) \quad (10)$$

In addition, because the parameters are unknown, the maximum likelihood method is used to estimate parameters including μ and σ (Zhao et al., 2016).

$$\mu = \frac{1}{N} \sum_{i=1}^N x_{\sigma i} = 0 \tag{11}$$

$$\sigma = \sqrt{\frac{1}{N} \sum_{i=1}^N (x_{\sigma i} - \bar{x})^2} = 3.80$$

We can find that the shadow fading of these paths conforms to a normal distribution with a mean of 0 regardless of the TX height. The shadow fading distribution of each path at different TX heights is as follows:

$$X_{\sigma} \sim \begin{cases} N(0, 3.80^2), \text{TX1} - \text{Route1} \\ N(0, 5.12^2), \text{TX1} - \text{Route2} \\ N(0, 5.54^2), \text{TX1} - \text{Route3} \\ N(0, 6.80^2), \text{TX1} - \text{Route4} \end{cases} \tag{12}$$

$$X_{\sigma} \sim \begin{cases} N(0, 2.09^2), \text{TX2} - \text{Route1} \\ N(0, 4.12^2), \text{TX2} - \text{Route2} \\ N(0, 5.33^2), \text{TX2} - \text{Route3} \\ N(0, 8.21^2), \text{TX2} - \text{Route4} \end{cases}$$

$$X_{\sigma} \sim \begin{cases} N(0, 3.14^2), \text{TX3} - \text{Route1} \\ N(0, 5.73^2), \text{TX3} - \text{Route2} \\ N(0, 4.90^2), \text{TX3} - \text{Route3} \\ N(0, 5.65^2), \text{TX3} - \text{Route4} \end{cases}$$

3.3 Delay Spread

Delay spread is a statistical variable, which is closely related to the radio wave propagation environment (time, region and user situation). It is a statistical description of the delay characteristics of multipath channels. The maximum and mean square values of delay spread are used to measure the time dispersion characteristics of the channel in multipath fading. The coherent bandwidth of the channel is its reciprocal, and the root-mean-square delay spread can be expressed as follows:

$$\sigma_{\tau} = \sqrt{\frac{\int_0^{+\infty} (\tau - \mu_{\tau})^2 P(\tau) d\tau}{\int_0^{+\infty} P(\tau) d\tau}} \tag{13}$$

μ_{τ} represents average delay, τ represents the delay, and μ_{τ} can be expressed as follows:

$$\mu_{\tau} = \frac{\int_0^{+\infty} \tau P(\tau) d\tau}{\int_0^{+\infty} P(\tau) d\tau} \tag{14}$$

Delay spread plays an important role in analysing the propagation characteristics of mm-wave. As shown in Figure 5, it presents the distribution of delay spread at different TX heights.

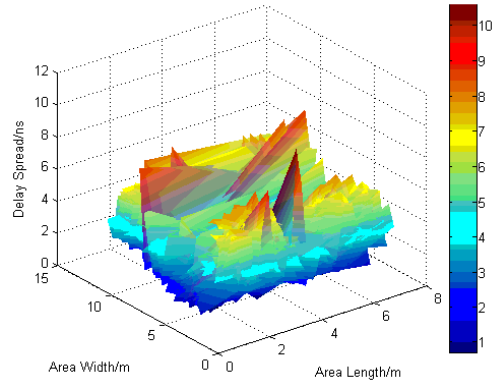


Figure 5(a): Distribution of delay spread at TX1.

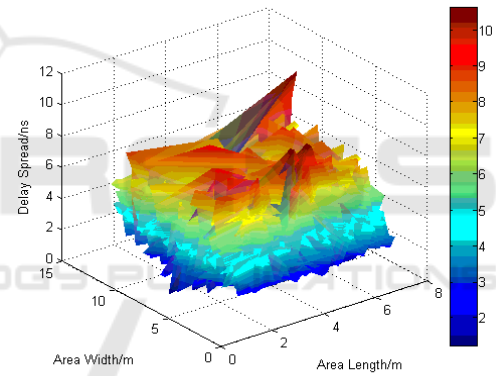


Figure 5(b): Distribution of delay spread at TX2.

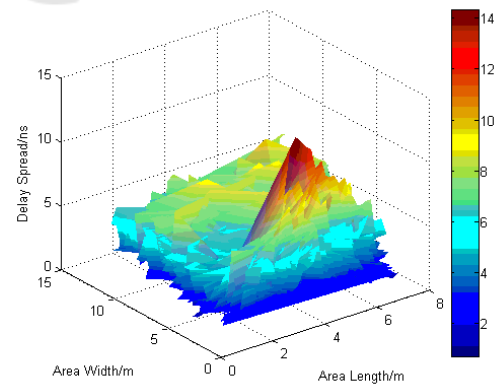


Figure 5(c): Distribution of delay spread at TX3.

By observing Figure 5, we can see that as the TX height increases, the spatial distribution of delay spread is not much different. The delay spread value is the smallest in the position without blockage. On the contrary, when there are blockages, such as a human body or a chair, the delay spread will increase correspondingly. Table 5 shows the maximum, minimum and mean of the delay spread in this meeting room at different TX heights. By analysing the data in the Table 5, we can find that the mean difference of delay spread at different height is very small. The maximum delay spread is basically the same when the TX height is 1.2m and 1.6m. But when the TX height is 2.2m, the maximum delay spread is 14.30ns, which is nearly 4ns larger than the former. In addition, as the TX height increases, there will be less blockage in the process of mm-wave propagation, and the delay spread value should be less. However, the mean delay spread increases with the increases of TX height. The main reason for this phenomenon may be that the TX height increases, which results in the increase of the distance between the TX and RX, so the delay spread value also increases.

Table 5: Delay spread at different height.

	Maximum(ns)	Minimum(ns)	Mean(ns)
TX1	10.57	0.71	3.78
TX2	10.61	1.22	4.88
TX3	14.30	0.69	4.81

4 CONCLUSIONS

Mm-wave would play a very important role in the future wireless communication system. This paper analyses mm-wave propagation characteristics at 28GHz in a crowded meeting room scenario. We create the simulation scenario by Wireless InSite and carry out simulation by SBR method. The result shows that Route3 path loss factor n is always larger than other routes regardless of TX height. Route 2 path loss factor n is less than freedom space path loss factor ($n=2$) due to line-of-sight path. In addition, we find that with the increase of TX heights, all Route1-4 $PL(d_0)$ are increased, And path loss factor n are decreased. All routes shadow fading obey the normal distribution with a mean of 0. When there are blockages, such as some human bodies or chairs, the delay spread will increase correspondingly. This paper provides a theoretical guiding for the design of wireless communication system in a crowded indoor environment.

ACKNOWLEDGMENTS

This paper is supported by the Joint Funds of National Natural Science Foundation of China (U1504604).

REFERENCES

- Bai, T., Ashwin, S., Ozge, K., Li J., 2018. Modeling and combating blockage in millimeter wave systems. *IEEE SigPort*.
- Bile, P., Sebastian, R., Dennis, M., et al., 2018. Statistical Characteristics Study of Human Blockage Effect in Future Indoor Millimeter and Sub-millimeter Wave Wireless Communications.
- Chahat, N., Zhadobov, M., Augustine R., et al., 2011. Human skin permittivity models for millimetre-wave range. *Electronics Letters*, 47(7), 427.
- Gapeyenko, M., Samuylov, A., Gerasimenko, M., Moltchanov, D., et al., 2016. Analysis of human-body blockage in urban millimeter-wave cellular communications. *IEEE International Conference on Communications*.
- Harmer, S. W., Rezugui, N., Bowring, N., Luklinska, Z., Ren, G., 2008. Determination of the complex permittivity of textiles and leather in the 14–40 GHz millimetre-wave band using a free-wave transmittance only method. *Iet Microwaves Antennas & Propagation*, 2(6), pp. 606-614.
- Islam, M. N., Subramanian, S., Partyka, A., et al., 2016. Coverage and capacity of 28 GHz band in indoor stadiums, *IEEE Wireless Communications and Networking Conference, Doha*, pp. 1-7.
- Maccartney, G. R., Deng, S., Sun, S., Rappaport, T. S., 2017. Millimeter-Wave Human Blockage at 73 GHz with a Simple Double Knife-Edge Diffraction Model and Extension for Directional Antennas. *IEEE Vehicular Technology Conference*.
- Nakamura, M., Sasaki, M., Kita, N., Takatori, Y., 2017. Path loss model in crowded areas considering multiple human blockage at 4.7 and 26.4 GHz. *IEEE Conference on Antenna Measurements & Applications (CAMA)*. pp. 40-43.
- Zhao, H., Yao, H., Guo, S., 2016. Research on path loss and shadow fading of ultra wideband simulation channel. *International Journal of Distributed Sensor Networks*. vol. 12, no.12, pp. 1-7.